Simulating Corrosion in a Crevice of Commercial Pure Titanium

Guigen Zhang[*,1,3,4]
[1] Department of Bioengineering, Clemson University, Clemson, SC 29634
[2] Department of Electrical and Computer Engineering, Clemson, SC 29634
[3] Institute for Biological Interfaces of Engineering, Clemson University, Clemson, SC 29634
[*]401 Rhodes Engineering Research Center, Clemson University, Clemson, SC 29634
guigen@clemson.edu

Abstract: More and more evidence from the clinically retrieved implants shows that corrosion in the crevices of modular implants is one major contributing factor leading to their failure. While implant corrosion has been investigated for many years, the true cause for modular implant failure remains elusive, thus hindering not only the clinical successes of these modular implants but also the regulatory approval processes. This work uses a computational approach with COMSOL to examine the corrosive process in a crevice of a commercial pure Titanium based on thermodynamics by considering simultaneously key electrode reactions, equilibrium reactions and mass transport, coupled with electrochemical polarization.

Keywords: Titanium, crevice corrosion, pH drop, modular metallic implants, computational modeling

1. Introduction

To allow maximum flexibility during surgery for surgeons to pick and choose different combinations of parts, implant modularity has been a common practice over the years. Modular metallic implants consist of not only different parts but different alloys as well. While implant modularity indeed provides great flexibility to improve personalized fits for patients, different parts coming together will create small gaps (or crevices) between parts and different alloys will cause galvanic potential differences.

Clinically retrieved implants reveal that corrosion in the crevices of these modular implants is indeed a server problem. The fretting motion between the parts and the coupled corrosive processes in a confined crevice with poor mas transport surely would accelerate the material deterioration of these implants. While fretting and crevice corrosion have been investigated for years both experimentally and computationally, the true cause for modular implant failure remains elusive.

Without knowing the underlying mechanisms, it is difficult, if not impossible, to solve the issue and improve the clinical success rates of these modular implants. Moreover, it poses challenges to the regulatory approval processes. For example, should the ionic concentration and pH in a crevice be monitored, and if so, how are the measurements related to the underlying corrosion process?

The main objective of this study is to take the first step to fundamentally reexamine the corrosive process in a crevice as a preparation for future study of compounded fretting and crevice corrosion. More specifically, it aims to: 1) examine the corrosive process in a crevice of a commercial pure Titanium based on thermodynamics by considering simultaneously key electrode reactions, equilibrium reactions and mass transport, coupled with electrochemical polarization, and 2) quantitatively evaluate the pH profile along the depth of a crevice with various different crevice widths and under various electrode potentials.

2. The Underlying Electrochemical Processes

A typical electrochemical process involves electrode kinetics (governed by the Butler-Vomer equation) and mass transport (by the Nernst-Planck equation). In this study, the electrode kinetics is activated by an

electrochemical polarization process. Fig. 1 shows a recorded polarization curve for commercial pure Titanium (cpTi). As in any typical polarization experiment, there are two regions: one in which the current is positive or anodic and the other where the current is negative or cathodic. Since in a typical polarization curve the current is often plotted in a log scale, an easy way to note the anodic and cathodic current regions is to split the curve into two branches by a horizontal divide where the current becomes negligible (this dividing line sometimes is referred to as the potential of zero current). In this way, the upper branch is the anodic region and the lower branch the cathodic region.

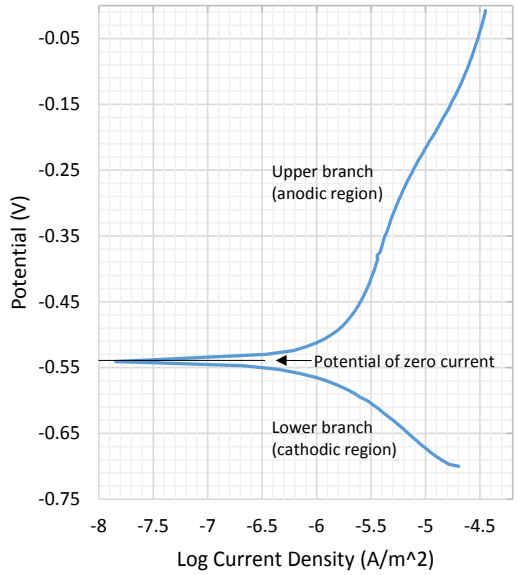

Fig. 1. Measured polarization curve used in this study.

2.1. Electrode reactions

To simplify matters, two main electrode reactions are considered under this polarization: the dissolution or oxidation of cpTi and the reduction of oxygen, as follows:

Oxidation:

$$Ti \rightarrow Ti^{4+} + 4e^{-} \quad (1)$$

Reduction:

$$O_2 + 4H^{+} + 4e^{-} \rightarrow 2H_2O \quad (2)$$

The oxidation reaction describes the process of metal dissolution into metallic ions and electrons. Because this reaction generates electrons, a favorite condition for it to occur is in the anodic region in which electrons are being pulled away (when current is positive). The reduction reaction describes the oxygen reduction process to consume the electrons in order to keep the whole-cell electrochemical process going. This reaction mainly takes place in the cathodic region in which electrons are being supplied (when current is negative).

2.2. Equilibrium reactions

Aside from the kinetically driven electrode reactions, there are several equilibrium reactions going on in the solution for the products of the electrode reactions. For example, the dissolved cpTi ions further react with water in the forms of following four equilibrium reactions:

$$Ti^{4+} + H_2O \leftrightarrow Ti(OH)^{3+} + H^{+} \quad (3)$$

$$Ti(OH)^{3+} + H_2O \leftrightarrow Ti(OH)_2^{2+} + H^{+} \quad (4)$$

$$Ti(OH)_2^{2+} + H_2O \leftrightarrow Ti(OH)_3^{+} + H^{+} \quad (5)$$

$$Ti(OH)_3^{+} + H_2O \leftrightarrow Ti(OH)_4 + H^{+} \quad (6)$$

To balance the pH of the aqueous solution, the equilibrium reaction of water dissociation is also considered:

$$H_2O \leftrightarrow OH^{-} + H^{+} \quad (7)$$

All these reactions occur in both directions in a state of dynamic equilibrium. Favorability of either forward or backward reactions is determined by the ratio of the product concentrations to reactant concentrations. Often one expresses this ratio in the form of equilibrium reaction constant, *K* (or sometimes as log*K*) as follows:

$$K = \frac{[G]^g[H]^h}{[A]^a[B]^b} \quad (8)$$

for a simple equilibrium reaction in the following form:

$$aA + bB \leftrightarrow gG + hH \quad (9)$$

When $K > 1$, the reaction favors the products and when $K < 1$ it favors the reactants.

For the five equilibrium equations considered here, the following values for the reaction constant are used to represent a 37°C simulated body fluid environment: log$K$ = -1.4, -1.7, -2.0, -4.0 and -13.6, respectively, for reactions (3) through (7).

3. The Mass Transport Process

The mass transport of all mobile species is governed by the Nernst-Planck equation, in which diffusion, electro-migration and convective driven mass transport under the thermodynamic laws of conservation of mass, momentum and energy are considered, as follows

$$\frac{\partial c_i}{\partial t} + \nabla \cdot (D_i \nabla c_i - z_i \mu_{m,i} F c_i \nabla \Phi) + u \cdot \nabla c_i = R_i \quad (10)$$

where D_i, c_i, z_i, $\mu_{m,i}$ and R_i are diffusion coefficient, concentration, valence charge, mobility, and source terms, respectively for each species (i) in the solution, and F, Φ and u are the Faraday constant, velocity and electrolyte potential, respectively. Note that convection is ignored in this study due to its absence ($u = 0$).

For the transport process, ten chemical species (i =1, 2, …, 10) are considered, including supporting electrolytes (NaCl): Na^+, Cl^-, Ti^{4+}, O_2, $Ti(OH)^{3+}$, $Ti(OH)_2^{2+}$, $Ti(OH)_3^+$, $Ti(OH)_4$, H^+ and OH^-. Table 1 lists their coefficient of diffusion. Note that the mobility for each species is determined by the Nernst-Einstein relation: $\mu_{m,i} = D_i/RT$ in which R is the gas constant and T is temperature in Kelvin.

Table 1. Diffusion coefficients used in this study

Species index (i)	Species	D_i ($\times 10^{-9}$ m^2/s)
1	Na^+	1.79
2	Cl^-	2.72
3	Ti^{4+}	0.91
4	O_2	1.97
5	$Ti(OH)^{3+}$	0.95
6	$Ti(OH)_2^{2+}$	0.98
7	$Ti(OH)_3^+$	1.00
8	$Ti(OH)_4$	1.07
9	H^+	12.46
10	OH^-	0.95

4. Modeling Consideration

With a computational modeling approach using COMSOL, a crevice is considered to be 10 mm in length with various widths: e.g., 10, 25 and 50 µm. For the solution, to simulate a simulated body environment, a supporting electrolyte of 0.9% NaCl (0.154 M) solution of pH 6.3 at 37°C is used. For the molar concentration of dissolved oxygen in bulk solution, it is calculated from the oxygen solubility (0.03 ml/l/mmHg) under a partial pressure of 100 mmHg along with oxygen density of 1.429 g/l, namely 0.134×10^{-3} mol/l. Thus this constant oxygen concentration is assumed and maintained at crevice mouth.

In the model, the polarization potential is swept from -0.7 V to -0.1 V while the oxygen reduction is considered in the cathodic current region and the cpTi oxidation considered in the anodic current region. Form the model, the resulting distribution profiles for various species, particularly the pH and concentration of O_2 and Ti^{4+}, inside the crevice along the depth of the crevice at various anodic and cathodic conditions are evaluated.

5. Results and Discussion

5.1 pH profile inside the crevice

Fig. 2 shows some selected results for the pH profiles under various polarization potentials and crevice widths conditions along the crevice depth. Note that all these plots are presented

with the horizontal axis in log scale - the left side represents the crevice mouth at a solution pH of 6.3 and the right side is the crevice tip.

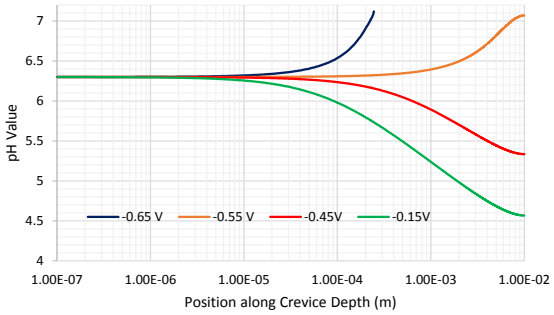

(a)

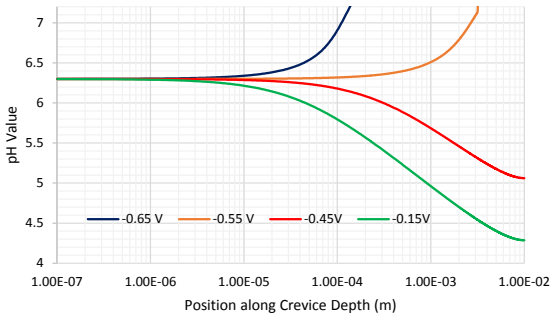

(b)

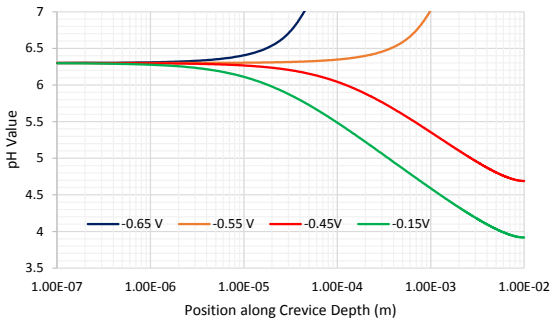

(c)

Fig. 2. The obtained pH profiels along crevice depth for various potential cases for (a) 50 µm crevice width, (b) 25 µm width, and (c) 10 µm width.

Fig. 2(a) shows the results for the case with 50 µm crevice width. At the two polarization potentials that produce cathodic current, namely -0.65 V and -0.55 V, the pH level increases as it goes deep into the crevice. This is so because under these potentials, protons are consumed according to Fig.1 and Eq. (2), making the crevice less acidic. When the potential is in the region that produces anodic current, e.g., -0.45 V and -0.15 V, the pH level decreases along the crevice depth. For example, at -0.15 V, the pH drops from 6.3 at the crevice mouth to 4.6 at the tip.

This general trend remains the same for the cases with different crevice widths, as one can see in Figs. 2(a) through 2(c), except that the level of pH differs at a given position along the crevice. For instance, under a polarization potential of -0.55 V (for producing cathodic current), the location that pH reaches to 7 is 7.3 mm, 2.7 mm and 1.0 mm into the crevice for the cases of 50 µm, 25 µm and 10 µm crevice widths, respectively. This result may be attributed to the fact that more oxygen is diffused into the crevice when the width of the crevice is larger, leading to more oxygen reduction and hence more proton consumption.

On the other hand, under a polarization potential for producing anodic current, the drop in pH becomes more server as the width decreases. For example, at -0.15 V, the pH at the tip reaches as low as 4.6, 4.3 and 3.9, respectively, for the cases of 50 µm, 25 µm and 10 µm crevice widths.

5.2 Oxygen concentration in the crevice

Fig. 3 shows the profiles for oxygen concentration inside the crevice under cathodic potentials.

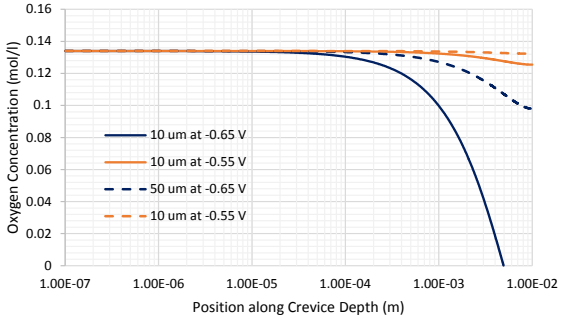

Fig. 3. The profiels for oxygen concentration along crevice depth for cases of 10 µm and 50 µm widths at -0.65V and -0.55 V.

Recall that the oxygen level inside the crevice is initially set as the same as that at the crevice mouth which is at a constant level. So in all cases, oxygen concentration decreases as it gets deeper into the crevice. The decrerase is more prominent in a narrower crevice, due to limited oxygen diffusion into the crevice when the width gets narrower.

5.3 Concentration of Ti ions in the crevice

Fig. 4 shows the concentration profiles for dissolved Titanium ions (Ti^{4+}) under a polarization potential of -0.15 V. The narrower the crevice is the higher the ion level becomes at the tip of the crevice. Particularly in a narrow crevice of 10 µm, metal dissolution can cause an increase in Ti^{4+} ions from a negligible level to as high as close to 1 µmol/l.

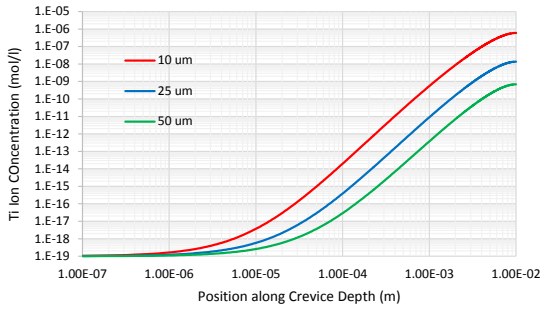

Fig. 4. The obtained Ti^{4+} concentration profiles along crevice depth for various width cases at -0.15V.

Although the corrosive environment considered here is under forced polarization, rather than a spontaneous process, the results shown here indicate that the thermodynamics in a tight space with poor mass transport could lead to severe pH drop when the anodic current condition is favored. This in turn can accelerate the corrosive process, leading to possible compounded device failure and tissue damage.

6. Conclusions

The obtained results shed some new insight into the mechanisms and consequences of crevice corrosion in commercial pure Titanium due to thermodynamics. Under an anodic condition, the pH value in a crevice can drop very severely, especially when the width of the crevice is small. Such a significant drop in pH will only accelerate the corrosive process, leading to compounded device failure and tissue damage. For improving the clinical successes of these modular implants and their regulatory approval processes, this work calls for the need of quantitatively analyzing the crevice environment in terms of reaction kinetics, mass transport, and the concentration of various relevant ions.

7. References

1. Crevice corrosion of iron in an Acetic Acid / Sodium Acetate solution. COMSOL tutorial.

2. Yaya K. et al. Numerical simulations study of the localized corrosion resistance of AISI 316L stainless steel and pure titanium in a simulated body fluid environment. Corrosion Science, 53, 3309-3314, 2011.

3. Brown S and Merritt K. Fretting corrosion of plates and screws: an in vitro test method. ASTM STP 859, 105-116, 1985.

4. Gilbert J and Jacobs J. The mechanical and electrochemical process associated with taper fretting crevice corrosion: a review. ASTM STP 1310. 1997.

8. Acknowledgement

The use of Clemson's Palmetto Cluster computing resources and the supports from Clemson Bioengineering and the Institute for Biological Interfaces of Engineering make this work possible. Also the helpful and informative discussions with Edmund Dickinson at COMSOL are appreciated.